Available online at www.sciencedirect.com
SCIENCE DIRECT®
PERGAMON
Polyhedron 22 (2003) 2877–2883
POLYHEDRON
www.elsevier.com/locate/poly

Chiral macrocyclic lanthanide complexes derived from (1*R*,2*R*)-1,2-diphenylethylenediamine and 2,6-diformylpyridine

Jarosław Mazurek, Jerzy Lisowski *

Department of Chemistry, University of Wrocław, 14 F. Joliot-Curie Street, Wrocław PL-50 383, Poland

Received 27 January 2003; accepted 22 May 2003

Abstract

The enantiopure complexes $[LnL]Cl_3 \cdot nH_2O$ ($Ln = La^{3+}$, Ce^{3+} and Eu^{3+}) of the new chiral macrocycle derived from (1*R*,2*R*)-1,2-diphenylethylenediamine and 2,6-diformylpyridine have been synthesised. The complexes have been characterised by NMR spectroscopy and mass spectrometry. The ^1H and ^{13}C signal assignment has been based on COSY, NOESY and HMQC measurements. The X-ray crystal structure of the $[CeL]Cl_3 \cdot 4H_2O$ complex has been determined. The cerium(III) ion is coordinated by six nitrogen atoms of the macrocyclic ligand and three chloride anions. The macrocycle in this complex adopts a relatively flat, twist-bent conformation.

Keywords: Macrocycles; Lanthanide complexes; Chiral complexes; NMR

1. Introduction

The Schiff bases obtained in a template 2+2 condensation of diamines and 2,6-diformylpyridine or 2,6-diacetylpyridine are particularly suitable for the coordination of relatively large metal ions [1]. The complexes of these hexaazamacrocyles with lanthanide(III) ions have attracted attention as efficient catalysts for the cleavage of the phosphate ester bond [2,3], as potential MRI contrast agents [4] and markers for biological systems [5–7].

When a chiral diamine is used in the above template reaction, chiral complexes can be obtained. In the case of the (1*R*,2*R*)-1,2-diaminocyclohexane precursor, enantiopure lanthanide(III) complexes (Fig. 1) $[LnL^1](NO_3)_3 \cdot nH_2O$ (where Ln is the lanthanide(III) ion) are formed [8–11]. The coordination of the lanthanide(III) ion in a chiral macrocyclic environment leads to interesting properties of these compounds. Thus, the $[TbL^1](NO_3)_3$ and $[EuL^1](NO_3)_3$ complexes have been shown to exhibit circularly polarised luminescence [8] and the paramagnetic $[EuL^1](NO_3)_3$ and $[YbL^1](NO_3)_3$ complexes have been shown to form diastereoisomeric complexes with D- and L-aminoacids [9].

Since the chiral, enantiopure complexes of hexaazamacrocycles are rare [6–13], and chiral macrocyclic lanthanide(III) complexes are promising candidates for enantioselective catalysts [14,15], we are interested in new complexes of this type. Here we present the study of enantiopure La(III), Ce(III) and Eu(III) complexes of the new ligand L (Fig. 1) derived from (1*R*,2*R*)-1,2-diphenylethylenediamine and 2,6-diformylpyridine. The complexes of the macrocycle L are related to the intensively studied complexes of the achiral ligand L^2 (Fig. 1) [1–4,16,17]. The lanthanide complexes of the latter macrocycle and of other pyridine derived hexaazamacrocycles may exhibit right or left helical twist of the two pyridine fragments. In the case of complexes of ligand L, however, the presence of the chiral centers in the diamine fragment leads to formation of complexes with the same direction of helical twist.

* Corresponding author. Tel.: +48-71-3757-252; fax: +48-71-3282-348.
E-mail address: jurekl@wchuwr.chem.uni.wroc.pl (J. Lisowski).

0277-5387/03/$ - see front matter © 2003 Elsevier Ltd. All rights reserved.
doi:10.1016/S0277-5387(03)00406-6

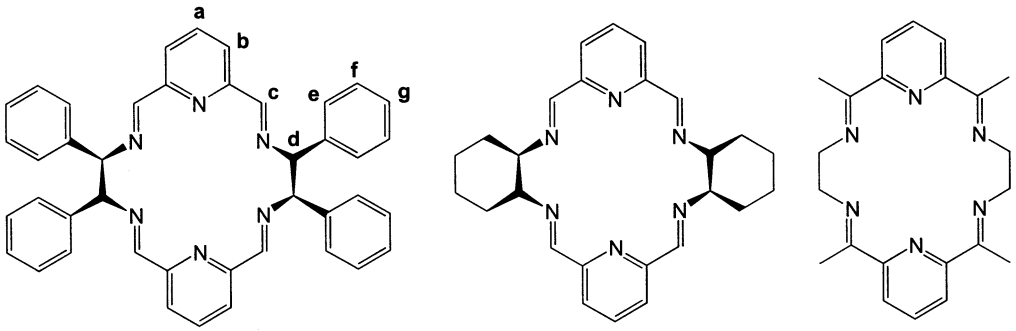

Fig. 1. The general structure and the labelling scheme of the macrocycle L and related ligands L^1 and L^2.

2. Experimental

2.1. Synthesis

Methanol was distilled over magnesium. All other reagents (Aldrich) were reagent grade and used as received. [LaL]$Cl_3 \cdot 3H_2O$: 2,6-diformylpyridine 67.5 mg (0.5 mmol), (1*R*,2*R*)-1,2-diphenylethylenediamine 106.1 mg (0.5 mmol) and lanthanum(III) chloride hexahydrate 88.3 mg (0.25 mmol) were refluxed in 10 ml of methanol for 3 h. The volume was reduced to 2 ml and the mixture was cooled down. The white product that formed was filtered, washed with methanol and dried in vacuum. Yield 65 mg, 28.2%. The [CeL]$Cl_3 \cdot 4H_2O$ and [EuL]$Cl_3 \cdot 6H_2O$ complexes have been prepared in similar way in 33% and 47% yields, respectively. All compounds gave satisfactory C, H, N analyses.

2.2. Methods

The NMR spectra were taken on Bruker Avance 500 and AMX 300 spectrometers. The chemical shifts were referenced to the residual solvent signal or TMS. The magnitude COSY spectra were acquired using $512 \times 1K$ data points. The data were processed by using a square sine bell window in both dimensions and zero filled to $1K \times 1K$ matrix. The phase-sensitive (TPPI) NOESY spectra were recorded using mixing times varying from 20 to 400 ms and shifted square sine function. The EXSY spectrum was obtained using a NOESY sequence with 3 ms mixing time. HMQC spectra were recorded using BIRD preparation period and 512×512 data points. A square sine function was used for apodization in both dimensions. Electrospray mass spectra were obtained using a Finnigan TSQ-700 instrument equipped with EST ion source. Elemental analyses were obtained from the elemental analyses facility in this department.

2.3. X-ray data collection

The crystals of [CeL]$Cl_3 \cdot 4H_2O$ were grown by slow evaporation of the chloroform+methanol solution of the complex. The crystal of approximately $0.4 \times 0.4 \times 0.3$ mm was mounted on a Kuma KM4 diffractometer equipped with a CCD counter and an Oxford Cryosystem low-temperature device. The measurement was performed at 100 K. The structure was solved with direct methods using SHELXS-97 [18] and least-squares full-matrix refinement were performed using SHELXL-97 [19]. The absorption correction was applied basing on refinement on *F* [20]. All of the hydrogen atoms were included geometrically, and their positions were constrained to the relevant C atoms, while their temperature factors were set at 1.2 times the trace of the C atoms. During refinement relatively high peaks ~ 2 e $Å^{-3}$ were found in the Fourier difference map and presumably result from disordered solvent. Details of the data collection are listed in Table 1. Publication and validation data were created using the WINGX program [21].

3. Results and discussion

3.1. X-ray crystal structure

The crystal structure of [CeL]$Cl_3 \cdot 4H_2O$ is built from layers. One layer is made from molecules of complex while the other one is made from distorted molecules of solvent i.e. water. Although it is likely that there are some interactions between layers, such as hydrogen bonds between chloride ions and water molecules, they can only be guessed because of strong disorder of the latter. The structure of [CeL]Cl_3 is composed of a macrocyclic complex and chloride anions connected to the central cerium (III) cation. The cerium cation has a nine-coordinate geometry (Fig. 2) that is very similar to that of the related complex [LaL^1]Cl_3 [11]. The coordination environment is composed of six nitrogen atoms belonging to the macrocycle (Ce–N distances in the

Table 1
Crystal data and structure refinement for $[CeL]Cl_3 \cdot 4H_2O$

Formula	$CeC_{42}H_{34}Cl_3N_6 \cdot 4H_2O$
F_w	941.22
T (K)	100(2)
λ (Å)	0.71073
Crystal system	triclinc
Space group	$P1$
Unit cell dimensions	
a (Å)	8.925(2)
b (Å)	9.566(2)
c (Å)	13.922(3)
α (°)	80.68(3)
β (°)	77.89(3)
γ (°)	67.55(3)
V (Å^3)	1069.7(4)
Z	1
D_{calc} (Mg m^{-3})	1.449
Absorption coefficient (mm^{-1})	1.298
$F(000)$	469
Crystal size (mm)	0.35 × 0.30 × 0.15
θ Range for data collection (°)	3.62–28.67
Index ranges	$-11 \le h \le 11$, $-12 \le k \le 12$, $-17 \le l \le 18$
Reflections collected	7537
Independent reflections	5799 ($R_{int} = 0.0293$)
Max. and min. transmission	0.7567 and 0.6439
Data/restraints/parameters	5799/3/502
Goodness-of-fit on F^2	1.042
Final R indices [$I > 2\sigma(I)$]	$R_1 = 0.0346$, $wR_2 = 0.0891$
R (all data)	$R_1 = 0.0348$, $wR_2 = 0.0892$
Absolute structure parameter	−0.007(11)
Largest difference peak and hole (e Å^{-3})	1.676 and −0.884

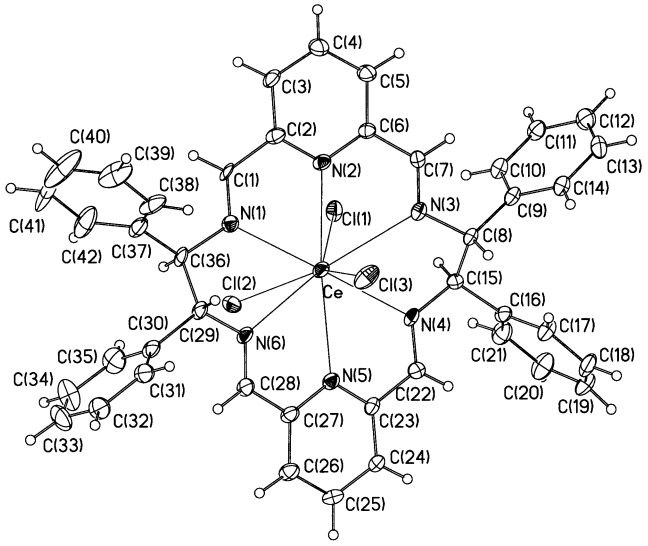

Fig. 2. View of the $[CeL]Cl_3 \cdot 4H_2O$ complex.

range 2.674(4)–2.800(4) Å) and three chloride anions (Ce–Cl distance vary from 2.800(2) to 2.855(2) Å). Selected bond lengths and angles are listed in Table 2. Two chloride anions are placed above and one below the mean plane of the macrocyclic ligand. The angles Cl(1)–Ce–Cl(2), Cl(2)–Ce–Cl(3) and Cl(1)–Ce–Cl(3) are 74.8(1)°, 144.3(1)° and 140.7(1)°, respectively.

Table 2
Bond lengths (Å) and bond angles (°) for $[CeL]Cl_3 \cdot 4H_2O$

Bond lengths			
Ce–N(1)	2.738(7)	Ce–N(2)	2.673(5)
Ce–N(3)	2.779(4)	Ce–N(4)	2.706(6)
Ce–N(5)	2.709(5)	Ce–N(6)	2.800(4)
Ce–Cl(1)	2.856(2)	Ce–Cl(2)	2.837(2)
Ce–Cl(3)	2.800(2)		
Bond angles			
Cl(1)–Ce–Cl(3)	140.7(1)	N(5)–Ce–N(6)	59.3(2)
Cl(1)–Ce–Cl(2)	74.8(1)	N(5)–Ce–N(3)	115.3(2)
Cl(2)–Ce–Cl(3)	144.2(1)	N(2)–Ce–Cl(3)	81.1(2)
N(1)–Ce–Cl(3)	87.3(2)	N(4)–Ce–Cl(3)	89.9(2)
N(3)–Ce–Cl(3)	74.7(1)	N(6)–Ce–Cl(3)	76.8(1)
N(5)–Ce–Cl(3)	83.6(2)	N(2)–Ce–Cl(2)	115.4(2)
N(1)–Ce–Cl(2)	75.8(2)	N(4)–Ce–Cl(2)	106.0(2)
N(3)–Ce–Cl(2)	140.9(1)	N(6)–Ce–Cl(2)	67.4(1)
N(5)–Ce–Cl(2)	77.3(1)	N(2)–Ce–Cl(1)	73.5(2)
N(1)–Ce–Cl(1)	104.9(2)	N(4)–Ce–Cl(1)	77.8(2)
N(3)–Ce–Cl(1)	66.8(2)	N(6)–Ce–Cl(1)	141.4(1)
N(5)–Ce–Cl(1)	119.7(2)	N(1)–Ce–N(2)	60.6(2)
N(1)–Ce–N(3)	120.5(2)	N(2)–Ce–N(4)	119.9(2)
N(1)–Ce–N(4)	177.1(2)	N(2)–Ce–N(3)	60.8(2)
N(2)–Ce–N(5)	164.7(2)	N(2)–Ce–N(6)	116.1(2)
N(1)–Ce–N(6)	59.2(2)	N(4)–Ce–N(5)	60.3(2)
N(3)–Ce–N(6)	151.6(2)	N(4)–Ce–N(3)	59.5(2)
N(5)–Ce–N(1)	118.4(2)	N(4)–Ce–N(6)	119.2(2)

The ligand L in the discussed complex adopts a twist-bend conformation, characteristic for complexes of hexaaza tetraimine macrocycles [1], similar to that of the ligand L^1 in the $[LaL^1]Cl_3$ complex [11]. The macrocyclic ligand in $[CeL]Cl_3 \cdot 4H_2O$ is only moderately twisted. The twist of the macrocycle can be measured by the torsion angle determined by C–N bonds of two pyridine rings C2–N2–N5–C27, equal to 14.1(2)°.

The macrocycle in $[CeL]Cl_3 \cdot 4H_2O$ is also only somewhat bent. The interplanar angle between pyridine rings (N2 C2 C3 C4 C5 C6 and N5, C23, C24, C25, C26, C27), reflecting both twisting and bending of the molecule, is 15.9(3)°, while the average value of the angle between the pyridine rings in related acrocyclic complexes is 47° [22]. Similarly, the angle between two planar sections defined by nine atoms from C36 through N2 to C8, and by nine atoms from C29 through N5 to C15 is 15.1(2)°, which is smaller than the average value of 45° observed for hexaaza tetraimine macrocycles [22]. Bending of the molecule influences also the angle determined by pyridine nitrogen atoms and the lanthanide ion, equal to 164.7(2)°. This value is similar to that of $[LaL^1]Cl_3$ (160.0°) [11] and $[LaL^2](NO_3)_3$ (164.3°) [16] complexes. It is, however, much larger than that of the $[CeL^2](NO_3)_3 \cdot 2H_2O$ complex (120.6°) [16]. This difference, however, does not have to correspond to different flexibility of the ligands L and L^2, but may result from the subtle differences in the steric interactions between

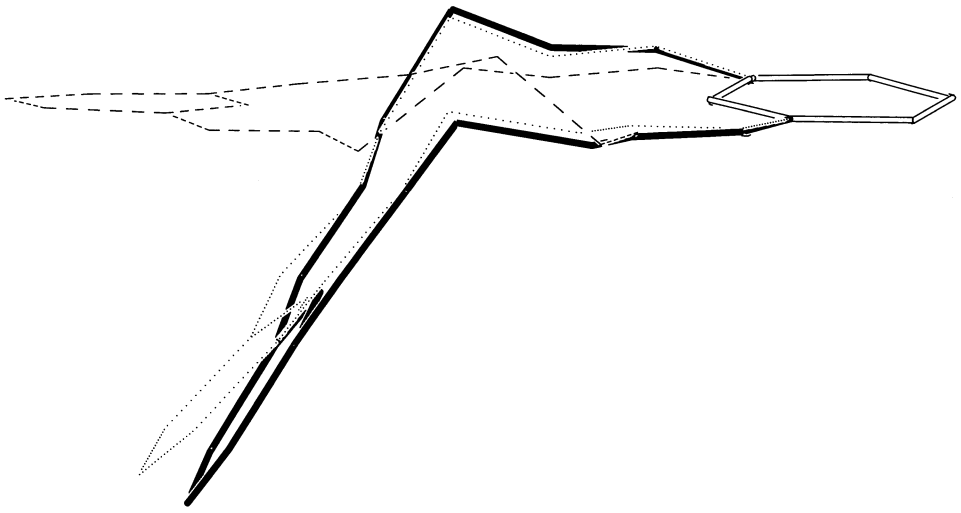

Fig. 3. The superposition of the conformations of macrocycle L in the $[CeL]Cl_3 \cdot 4H_2O$ complex (dashed line) and the $[EuL]Cl_3 \cdot 5H_2O$ complex (dotted line for the crystallographically independent molecule a, solid line for the molecule b). Phenylene rings and hydrogen atoms are omitted for clarity. The common part (open line) is one of the pyridine rings.

the macrocycle and the axial ligands. In fact the preliminary X-ray crystal structure of the $[EuL]Cl_3 \cdot 5H_2O$ complex,[1] although not sufficiently solved, clearly shows the considerably bent conformation of the ligand L in this complex (Fig. 3). This time the interplanar angle between the pyridine rings, which is 47.4(5)° and 59.4(5)° for the crystallographically independent molecules a and b in $[EuL]Cl_3 \cdot 5H_2O$, respectively, is much larger than that of 15.9(3)° for the Ce(III) complex. This difference reflects increased bending rather than twisting of the macrocycle, since the torsion angle determined by C–N bonds of the two pyridine rings, equal to 8(2)° and 17(2)° for the molecules a and b, respectively, is similar to that of the $[CeL]Cl_3 \cdot 4H_2O$ complex. The Eu(III) complex differs from the Ce(III) complex in axial coordination. In the former complex, in both crystallographically independent molecules, there are two water molecules and one chloride anion bound to the Eu(III). Since this axial ligand set is sterically less demanding than the set of three chloride anions of the Ce(III) complex, we suggest that the difference in geometry of the macrocycle is due to the smaller ion radius of Eu(III), rather than the different environment of the central ion.

[1] Crystal data of $[EuL(H_2O)_2Cl]Cl_2 \cdot 3H_2O$: monoclinic, space group $C2$, $Z = 8$, $a = 42.08(6)$ Å, $b = 17.295(11)$ Å, $c = 12.017(8)$ Å, $\beta = 95.80°$, $V = 8702(15)$ Å, $R_{int} = 0.081$ final $R = 0.092$, $R_w = 0.199$. Because of the low stability, the twinning of the crystal and significant disorder of the second coordination sphere (solvent and chloride ions), refinement was stopped with the anisotropic thermal parameters for Eu and Cl ions only, the rest of non-H atoms were refined isotropically.

3.2. Solution characterisation

The investigated compounds give rise to seven signals in their ^1H NMR spectra (the signals of aromatic protons are partially overlapped) and nine signals in ^{13}C NMR spectra. The spectra confirm the formation of the macrocyclic ligand and purity of the complexes. The spectra are somewhat concentration dependent, probably due to partial dissociation of chloride anions. The number of resonances indicates the effective D_2 symmetry of the $[LnL]Cl_3$ complexes in the investigated solutions. It should be noted that this symmetry is higher than that observed in the solid state. This difference may arise from the fast dynamic exchange of axial chloride anions and/or solvent molecules, that renders the two sides of the macrocycle equivalent, similarly as it was observed for the related macrocyclic lanthanide complexes derived from 1,2-diaminocyclohexane [11].

The spectra of the $[LaL]Cl_3$ complex can be easily assigned on the basis of chemical shift values (Table 3). The spectra of the $[CeL]Cl_3 \cdot 4H_2O$ and $[EuL]Cl_3 \cdot 6H_2O$ complexes differ from those of the La(III) complex due to the paramagnetic contribution to the chemical shift (isotropic shift). In general this contribution is difficult to predict on a theoretical basis [23–27], so the assignment of the spectra (Table 3) was confirmed by analysis of the COSY, NOESY, HMQC and HMBC spectra (see Fig. 4 for example). The COSY correlated signals of protons a and b (see. Fig. 1 for the labelling scheme) are easily identified on the basis of the integration of signal a (intensity 2H in contrast to intensity 4H for positions b, c, d and g and intensity 8H for positions e and f). The NOESY spectra allow to find the connectivities between the signals of protons a and b, b and c as well as c and e.

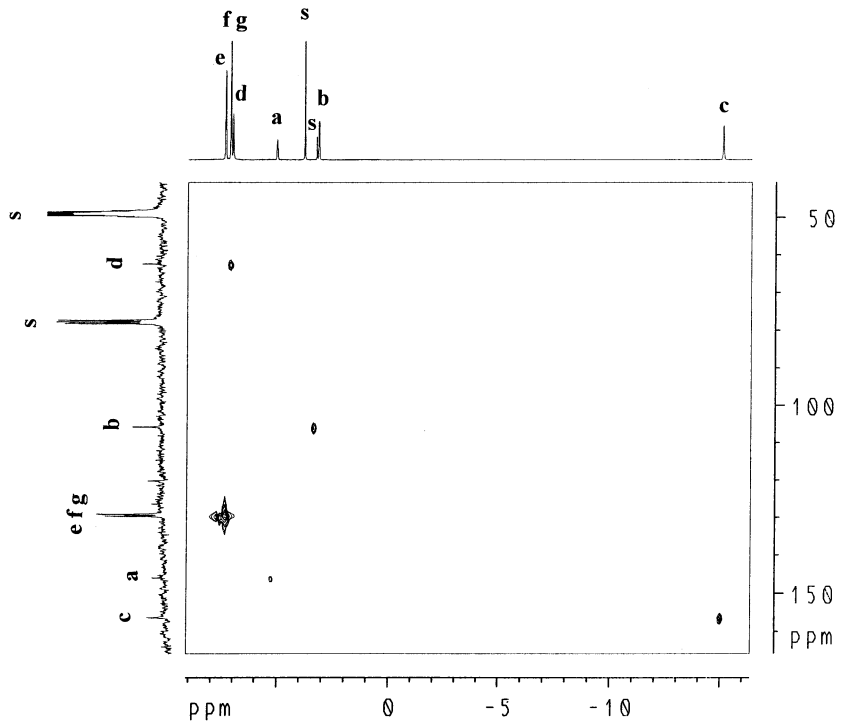

Fig. 4. The HMQC spectrum of $[EuL]Cl_3 \cdot 6H_2O$ ($CD_3OD/CDCl_3$ 1:2 v/v solution, 320 K), s—solvent and HDO signals.

The signal of proton e is COSY and NOESY correlated to overlapped phenyl ring signals f and g. The expected NOESY correlation between signals of protons c and d was not observed due to the line broadening.

The substantial differences in the chemical shifts of the La(III), Ce(III) and Eu(III) complexes, caused by the paramagnetic contribution in the case of $[CeL]Cl_3 \cdot 4H_2O$ and $[EuL]Cl_3 \cdot 6H_2O$ derivatives, clearly confirm the coordination of the lanthanide ion to the ligand L in solution. In general, the signals of the protons and carbon atoms that are close to the metal ion in terms of the distance or the number of connecting bonds, experience large paramagnetic shift, while the signals of the phenyl rings experience very small paramagnetic shift. In particular the −27.73 ppm value of isotropic (paramagnetic) shift observed for the azomethine proton c of $[EuL]Cl_3 \cdot 6H_2O$ falls in the range characteristic for this position in other Eu(III) macrocyclic complexes [9,11,28,29].

The identity of the complexes is also confirmed by electrospray ionisation mass spectrometry. For instance the ESI MS^+ of methanol/acetic acid solution of the

Table 3
^1H NMR and ^{13}C NMR chemical shifts of the $[LnL]Cl_3$ complexes (295 K, $CD_3OD/CDCl_3$ 1:2 v/v)

Complex	a	b	c	d	e	f	g		
^1H NMR									
$[LaL]Cl_3 \cdot 3H_2O$	8.18	7.76	8.16	5.82	7.23–7.32	7.23–7.32	7.23–7.32		
$[CeL]Cl_3 \cdot 4H_2O$	11.24	11.42	15.19	3.16	7.29	7.48	7.48		
$[EuL]Cl_3 \cdot 6H_2O$ [a]	4.42	2.27	−17.89	7.24	7.31	7.11	7.10		
$[EuL]Cl_3 \cdot 6H_2O$ [b]	4.17	1.81	−19.57	6.60	7.17	6.98	6.98		
$[PrL](AcO)^{2+}$	8.90	8.25	10.79	3.22	6.56	7.06	7.06		
$[EuL](AcO)^{2+}$	6.66	5.62	−10.72	11.76	9.18	8.01	7.91		
	a	b	c	d	e	f	g	C_{quat}	C_{quat}
^{13}C NMR									
$[LaL]Cl_3 \cdot 3H_2O$	142.29	130.41	165.31	75.51	130.41	129.82	129.51	153.03	135.51
$[CeL]Cl_3 \cdot 4H_2O$	146.85	138.36	171.68	74.75	130.58	130.08	129.78	169.93	137.42
$[EuL]Cl_3 \cdot 6H_2O$	145.85	103.16	154.07	60.84	129.54	129.07	129.07	121.70	118.71

[a] 300 K.
[b] CD_3OD.

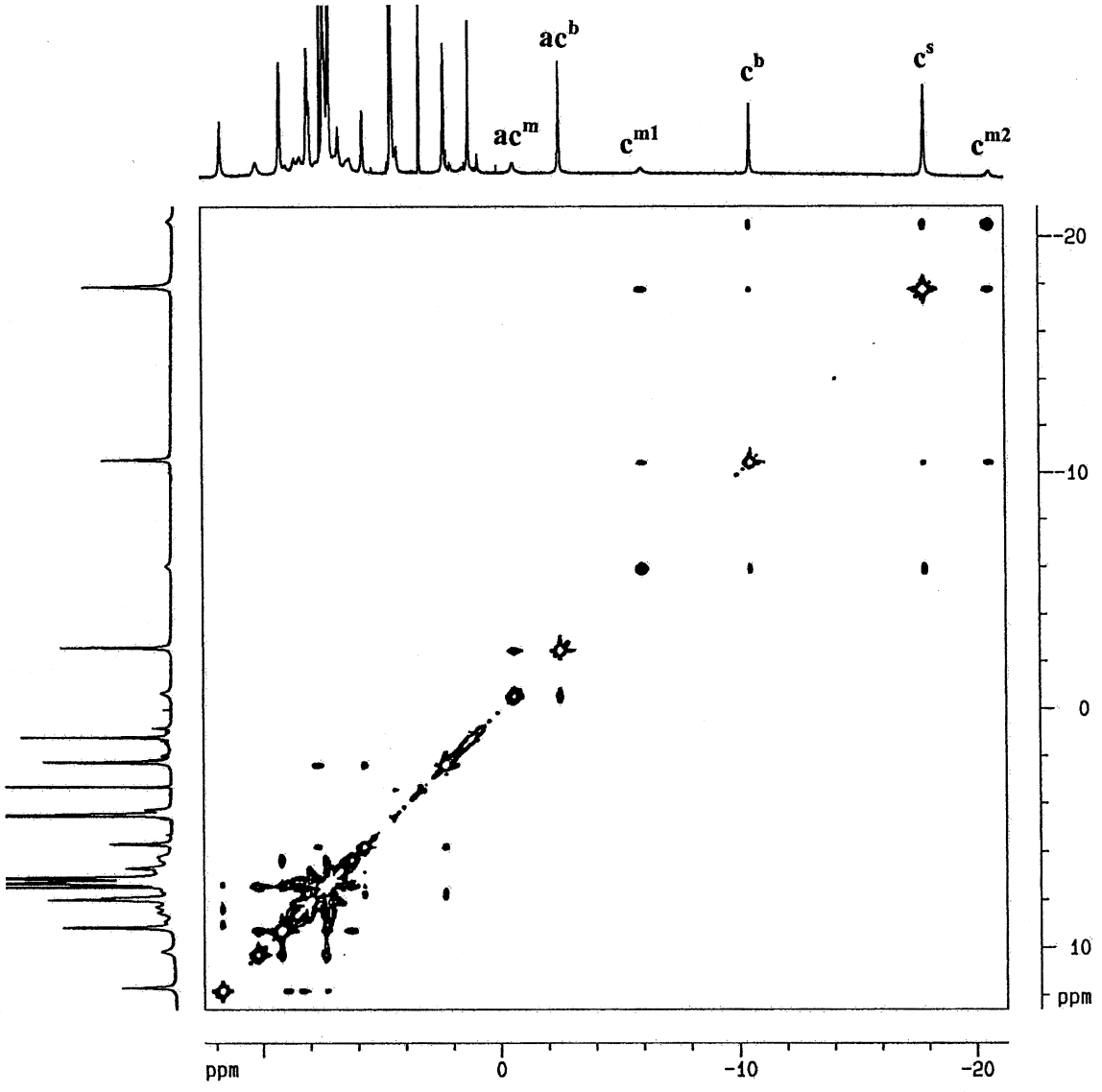

Fig. 5. The EXSY spectrum of $[EuL]Cl_3 \cdot 6H_2O$ with 0.63 equiv. of sodium acetate added ($CD_3OD/CDCl_3$ 1:2 v/v solution, 300 K). The c^s, c^b, c^{m1} and c^{m2} indicate the azomethine signals of the starting complex, the bisacetate complex and the two signals of monoacetate complex, respectively. ac^m and ac^b denotes the resonances of bound acetate anion in mono- and bisacetate complexes, respectively.

$[LaL]Cl_3$ complex gave peaks at *m/e* 410, 856 and 880 corresponding to ions $[LaL](AcO)^{2+}$, $[LaL](AcO)Cl^+$ and $[LaL](AcO)_2^+$, respectively. This result indicates that the bound chloride anions can be easily exchanged in solution for other axial ligands such as acetate.

The binding of acetate anion has been also observed with ^1H NMR spectroscopy, because the axial ligand (counteranion) has a profound influence on NMR spectra of paramagnetic macrocyclic lanthanide(III) complexes [9,28,30]. In the case of the Ce(III) complex, titration of the $[CeL]Cl_3 \cdot 4H_2O$ complex in $CD_3OD/CDCl_3$ 1:2 v/v solution with CD_3OD solution of sodium acetate results initially in broadening of signals of the starting complex and appearance of a new set of broad signals. When 2 or more equiv. of acetate are added the new signals become sharp. This behaviour is in accord with a dynamic process of intermediate exchange rate on the NMR timescale and formation of a bisacetate complex with effective D_2 symmetry. The ^1H NMR spectrum of the bisacetate complex can be assigned tentatively on the basis of linewidth analysis, integration, splitting pattern and comparison with the spectrum of the starting chloride complex (Table 3).

A more clear situation is observed in the case of NMR titration of the europium(III) complex, where a slow exchange limit is reached. In this case, addition of acetate to $[EuL]Cl_3 \cdot 6H_2O$ solution allows observation of both monoacetate and bisacetate complexes. The latter complex gives rise to 7 ^1H NMR signals in accord with the effective D_2 symmetry. The former complex corresponds to a spectrum with pairs of resonances b^1 and b^2, c^1 and c^2, etc. (Fig. 5). This doubling of the

number of resonances is due to C_2 symmetry of the mixed acetate/chloride complex. In such a complex the different axial coordination of the two sides of the macrocycle together with the helical twist of the ligand makes two halves of the macrocycle not equivalent. Similar doubling of the signals was observed before for the Yb(III) complexes of the ligand L^1 with the mixed axial coordination [31]. Interestingly, when 1 equiv. of acetate is added, the concetration of bisacetate complex is higher than the concentration of monoacetate complex, indicating the larger binding constant of the second acetate anion. When 2 or more equiv. of acetate are added, only the spectrum of the bisacetate derivative is observed. The above axial ligand exchange process is clearly seen in the EXSY spectrum (Fig. 5). In this way the signal assignment of the acetate complex can be safely based on the assignment of the starting $[EuL]Cl_3 \cdot 6H_2O$ (Table 3).

In conclusion, both solution NMR study and solid state X-ray crystal structure clearly show the formation of lanthanide(III) complexes of the new chiral macrocycle L. Presently we are investigating the interactions of these complexes with chiral molecules that can be bound in the axial positions.

4. Supplementary material

Crystallographic data for the structural analysis have been deposited with the Cambridge Crystallographic Data Centre, CCDC Nos. 201566 and 201567 for the compounds $[CeL]Cl_3 \cdot 4H_2O$ and $[EuL]Cl_3 \cdot 6H_2O$, respectively. Copies of this information may be obtained free of charge from The Director, CCDC, 12 Union Road, Cambridge, CB2 1EZ, UK (fax: +44-1223-336033; e-mail: deposit@ccdc.cam.ac.uk or www: http://www.ccdc.cam.ac.uk).

Acknowledgements

This work was supported by KBN grant 3 T09A 11519.

References

[1] V. Alexander, Chem. Rev. 95 (1995) 273.
[2] J.R. Morrow, L.A. Butterey, V.M. Shelton, K.A. Berback, J. Am. Chem. Soc. 114 (1992) 1903.
[3] R.W. Hay, N. Govan, Polyhedron 24 (1997) 4233.
[4] P.H. Smith, J.R. Brainard, D.E. Morris, G.D. Jarvinen, R.R. Ryan, J. Am. Chem. Soc. 111 (1989) 7437.
[5] L.M. Vallarino, R.C. Leif, US patent 5373093 (1994).
[6] F. Benetollo, G. Bombieri, A.M. Adeyga, K.K. Fonda, W.A. Gootee, K.M. Samaria, L.M. Vallarino, Polyhedron 21 (2002) 425.
[7] F. Benetollo, G. Bombieri, W.A. Gootee, K.K. Fonda, K.M. Samaria, L.M. Vallarino, Polyhedron 17 (1998) 3633.
[8] T. Tsubomura, K. Yasaku, T. Sato, M. Morita, Inorg. Chem. 31 (1992) 447.
[9] J. Lisowski, Magn. Reson. Chem. 37 (1999) 287.
[10] J. Lisowski, P. Starynowicz, Polyhedron 19 (2000) 465.
[11] J. Lisowski, J. Mazurek, Polyhedron 21 (2002) 811.
[12] L.H. Bryant, Jr, A. Lachgar, K.S. Coates, S.C. Jackels, Inorg. Chem. 33 (1994) 2219.
[13] P.M. Fitzsimmons, S.C. Jackels, Inorg. Chim. Acta 246 (1996) 301.
[14] S. Kobayashi, T. Hamada, S. Nagayama, K. Manabe, Org. Lett. 3 (2001) 165.
[15] H.C. Aspinall, Chem. Rev. 102 (2002) 1807.
[16] A.M. Arif, J.D.J. Backer-Dirks, C.J. Gray, F.A. Hart, M.B. Hursthouse, J. Chem. Soc., Dalton Trans. (1987) 1665.
[17] F. Benetollo, G. Bombieri, K.K. Fonda, L.M. Vallarino, Polyhedron 16 (1997) 1907.
[18] G.M. Sheldrick, SHELX-97: Programs for Crystal Structure Analysis (Release 97-2), Göttingen, Germany, 1998.
[19] G.M. Sheldrick, SHELX-76: Program for Crystal Structure Refinement, Göttingen, Germany, 1976.
[20] S. Parkin, B. Moezzi, H. Hope, J. Appl. Crystallogr. 28 (1995) 53.
[21] L.J. Farrugia, J. Appl. Crystallogr. 32 (1999) 837.
[22] Cambridge Structural Database, Conquest 1.0 version October 2002.
[23] I. Bertini, C. Luchinat, NMR of Paramagnetic Molecules in Biological Systems; Benjamin/Cummings, Menlo Park, CA, 1986.
[24] I. Bertini, P. Turano, A.J. Vila, Chem. Rev. 93 (1993) 2833.
[25] I. Bertini, C. Luchinat, Coord. Chem. Rev. 150 (1996) 1.
[26] A.D. Sherry, C.F.G.C. Geraldes, in: J.-C.G. Bunzli (Ed.), Lanthanide Probes in Life, Chemical and Earth Sciences. Theory and Practice, Ch. 4, Elsevier, Amsterdam, 1989.
[27] G.N. La Mar, W.DeW. Horrocks Jr., R.H. Holm (Eds.), NMR of Paramagnetic Molecules, Academic Press, New York, 1973.
[28] J. Lisowski, J.L. Sessler, V. Lynch, T.D. Mody, J. Am. Chem. Soc. 117 (1995) 2273.
[29] J. Lisowski, P. Starynowicz, Polyhedron 18 (1999) 443.
[30] K.K. Fonda, L.M. Vallarino, Inorg. Chim. Acta 334 (2002) 403.
[31] J. Lisowski, Presented at ISCD 12 Chirality 2000, Chamonix Mont-Blanc, September 2000.